

## Lattice-QCD Calculations of TMD Soft Function Through Large-Momentum Effective Theory

---

Qi-An Zhang,<sup>a,b,\*</sup> Jun Hua,<sup>c</sup> Yikai Huo,<sup>c</sup> Xiangdong Ji,<sup>b,d</sup> Yizhuang Liu,<sup>b</sup> Yu-Sheng Liu,<sup>b</sup> Maximilian Schlemmer,<sup>e</sup> Andreas Schäfer,<sup>e</sup> Peng Sun,<sup>f</sup> Wei Wang<sup>c</sup> and Yi-Bo Yang<sup>g</sup>

<sup>a</sup>*School of Physics, Beihang University, Beijing 102206, China*

<sup>b</sup>*Tsung-Dao Lee Institute, Shanghai Jiao Tong University, Shanghai 200240, China*

<sup>c</sup>*INPAC, SKLPPC, MOE KLPPC, School of Physics and Astronomy, Shanghai Jiao Tong University, Shanghai 200240, China*

<sup>d</sup>*Department of Physics, University of Maryland, College Park, MD 20742, USA*

<sup>e</sup>*Institut für Theoretische Physik, Universität Regensburg, D-93040 Regensburg, Germany*

<sup>f</sup>*Nanjing Normal University, Nanjing, Jiangsu, 210023, China*

<sup>g</sup>*CAS Key Laboratory of Theoretical Physics, Institute of Theoretical Physics, Chinese Academy of Sciences, Beijing 100190, China*

*E-mail: zhangqa@buaa.edu.cn*

The transverse-momentum-dependent (TMD) soft function is a key ingredient in QCD factorization of Drell-Yan and other processes with relatively small transverse momentum. We present a lattice QCD study of this function at moderately large rapidity on a 2+1 flavor CLS dynamic ensemble with  $a = 0.098$  fm. We extract the rapidity-independent (or intrinsic) part of the soft function through a large-momentum-transfer pseudo-scalar meson form factor and its quasi-TMD wave function using leading-order factorization in large-momentum effective theory. We also investigate the rapidity-dependent part of the soft function—the Collins-Soper evolution kernel—based on the large-momentum evolution of the quasi-TMD wave function.

*The 38th International Symposium on Lattice Field Theory, LATTICE2021 26th-30th July, 2021  
Zoom/Gather@Massachusetts Institute of Technology*

---

\*Speaker

## 1. Introduction

For high-energy processes such as Higgs production at the Large-Hadron Collider, quantum chromodynamics (QCD) factorization and parton distribution functions (PDFs) have been essential for making theoretical predictions [1, 2]. But for processes involving observation of a relatively small transverse momentum,  $Q_\perp$  such as in Drell-Yan (DY) production and semi-inclusive deep inelastic scattering, a new non-perturbative quantity called *soft function* is required to capture the physics of non-cancelling soft gluon-radiation at fixed  $Q_\perp$  [3–6]. Physically, the soft function in DY is a cross section for a pair of a high-energy quark and anti-quark (or gluon) traveling in the opposite light-cone directions to radiate soft gluons of total transverse momentum  $Q_\perp$  before they annihilate. Although much progress has been made in calculating the soft function in perturbation theory at  $Q_\perp \gg \Lambda_{\text{QCD}}$  [7, 8], it is intrinsically non-perturbative when  $Q_\perp$  is  $\mathcal{O}(\Lambda_{\text{QCD}})$ . Calculating the non-perturbative transverse-momentum-dependent (TMD) soft function from first principles became feasible only recently [9].

The main difference in such a calculation in lattice QCD is that it involves two light-like Wilson lines along directions  $n^\pm = \frac{1}{\sqrt{2}}(1, \vec{0}_\perp, \pm 1)$  in  $(t, \perp, z)$  coordinates, making direct simulations in Euclidean space impractical. However, much progress has been made in recent years in calculating physical quantities such as light-cone PDFs using the framework of large-momentum effective theory (LaMET) [10, 11]. The key observation of LaMET is that the collinear quark and gluon modes, usually represented by light-like field correlators [12–15], can be accessed for large-momentum hadron states. A detailed review of LaMET and its applications to collinear PDFs and other light-cone distributions can be found in Refs.[16, 17]. More recently, some of the present authors have proposed that the TMD soft function can be extracted from a special large-momentum-transfer form factor of either a light meson or a pair of quark-antiquark color sources [9]. Once calculated, the TMD factorization of the Drell-Yan and similar processes can be made with entirely lattice-QCD-computable non-perturbative quantities [18–23].

The TMD soft function is often defined and applied not in momentum space but in transverse coordinate space in terms of the Fourier transformation variable  $b_\perp$ . In addition, it also depends on the ultraviolet (UV) renormalization scale  $\mu$  (often defined in dimensional regularization and minimal subtraction or  $\overline{\text{MS}}$ ) and rapidity regulators  $Y + Y'$  [9, 12],

$$S(b_\perp, \mu, Y + Y') = e^{(Y+Y')K(b_\perp, \mu)} S_I^{-1}(b_\perp, \mu) \quad (1)$$

where the first factor is related to rapidity evolution [described by the Collin-Soper (CS) kernel  $K$ ], and the second factor  $S_I$  is the intrinsic, rapidity independent, part of the soft contribution. The rapidity-regulator-independent CS-kernel  $K$  is found calculable by taking ratio of the quasi-TMDPDF at two different momenta [20–25]. On the other hand, calculating the intrinsic soft function on the lattice has never been attempted before.

In this paper we present the first lattice QCD calculation of the intrinsic soft function  $S_I$  with several momenta on a 2+1 flavor CLS ensemble with  $a = 0.098$  fm [26], see Table I. In particular we perform simulations of the large-momentum light-meson form factor and quasi-TMD wave functions (TMDWFs), whose ratio gives the intrinsic soft function [9]. The Wilson loop matrix element will be used to remove the linear divergence in the quasi-TMD wave function. The CS kernel,  $K$ , can also be calculated from the external momentum dependence of the quasi-TMD wave

function [16], and we will calculate it as a by-product. Our result is consistent with that of quenched lattice calculations of TMDPDFs [25].

## 2. Theoretical Framework

The intrinsic soft function ( $S_I$ ) can be obtained from the QCD factorization of a large-momentum form factor of a non-singlet light pseudo-scalar meson with constituents  $\pi = \bar{q}_2 \gamma_5 q_1$ , with the transition current made of two quark-bilinears with a fixed transverse separation  $\vec{b} = (\vec{n}_\perp b_\perp, 0)$ ,

$$F(b_\perp, P^z) = \langle \pi(-\vec{P}) | (\bar{q}_1 \Gamma q_1)(\vec{b})(\bar{q}_2 \Gamma q_2)(0) | \pi(\vec{P}) \rangle_c. \quad (2)$$

Here  $q_{1,2}$  are light quark fields of different flavors, and  $\vec{P} = (\vec{0}_\perp, P^z)$ . To extract the soft-factor, as pointed out in Ref. [9], one can choose different quark flavors for the operators and mesonic states in the above equation. The benefit of this choice is only connected currents will contribute to the contractions in above form factor, thus a subscript  $c$  is added on the right-hand side of Eq. (2). By construction, the disconnected insertion is not relevant in this scenario which we will adopt in this work.

It can be shown that the form factor defined in Eq. (2) is factorizable into the quasi-TMDWF  $\Phi$  and the intrinsic soft function  $S_I$  [9, 16]

$$F(b_\perp, P^z) = S_I(b_\perp) \int_0^1 dx dx' H(x, x', P^z) \Phi^\dagger(x', b_\perp, -P^z) \Phi(x, b_\perp, P^z), \quad (3)$$

where  $H$  is the perturbative hard kernel. The quasi-TMDWF  $\Phi$  is the Fourier transformation of the coordinate-space correlation function

$$\phi(z, b_\perp, P^z) = \lim_{\ell \rightarrow \infty} \frac{\phi_\ell(z, b_\perp, P^z, \ell)}{\sqrt{Z_E(2\ell, b_\perp)}}, \quad (4)$$

$$\phi_\ell(z, b_\perp, P^z, \ell) = \left\langle 0 \left| \bar{q}_1 \left( \frac{z}{2} n^z + \vec{b} \right) \Gamma_\Phi \mathcal{W}(\vec{b}, \ell) q_2 \left( -\frac{z}{2} n^z \right) \right| \pi(\vec{P}) \right\rangle. \quad (5)$$

In the above  $\mathcal{W}(\vec{b}, \ell)$  is the spacelike staple-shaped gauge link,

$$\begin{aligned} \mathcal{W}(\vec{b}, \ell) = & \mathcal{P} \exp \left[ i g_s \int_{-\ell}^{z/2} ds n^z \cdot A(n^z s + b_\perp) \right] \times \mathcal{P} \exp \left[ i g_s \int_0^{b_\perp} ds n_\perp \cdot A(-\ell n^z + s n_\perp) \right] \\ & \times \mathcal{P} \exp \left[ i g_s \int_{-z/2}^{-\ell} ds n^z \cdot A(n^z s) \right], \end{aligned} \quad (6)$$

$n^z$  and  $n_\perp$  are the unit vectors in  $z$  and transverse directions respectively.  $Z_E(2\ell, b_\perp)$  is the vacuum expectation value of a rectangular spacelike Wilson loop with size  $2\ell \times b_\perp$  which removes the pinch-pole singularity and Wilson-line self-energy in quasi-TMDWF [9].

Since the UV divergence of intrinsic soft function obtain the multiplicative renormalization [16], the ratio  $S_I(b_\perp, 1/a)/S_I(b_{\perp,0}, 1/a)$  calculable on lattice is UV renormalization-scheme independent, where  $b_{\perp,0}$  is a reference distance which is taken small enough to be calculated perturbatively. Thus we can obtain the result in the  $\overline{\text{MS}}$  scheme through

$$S_{I,\overline{\text{MS}}}(b_\perp, \mu) = \left( \frac{S_I(b_\perp, 1/a)}{S_I(b_{\perp,0}, 1/a)} \right) S_{I,\overline{\text{MS}}}(b_{\perp,0}, \mu) \quad (7)$$

where  $S_{I,\overline{\text{MS}}}(b_{\perp,0}, \mu)$  is perturbatively calculable, e.g.,

$$S_{I,\overline{\text{MS}}}(b_{\perp}, \mu) = 1 - \frac{\alpha_s C_F}{\pi} \ln \frac{\mu^2 b_{\perp}^2}{4e^{-2\gamma_E}} + O(\alpha_s). \quad (8)$$

In the present exploratory study, we will consider only leading order matching in Eq. (3), for which the perturbative kernel is  $H(x, x', P^z) = 1/(2N_c) + O(\alpha_s)$ , independent of  $x$  and  $x'$ . Using  $\phi(0, b_{\perp}, -P^z) = \phi(0, b_{\perp}, P^z)$  under parity transformation, we obtain

$$S_I(b_{\perp}) = \frac{2N_c F(b_{\perp}, P^z)}{|\phi(0, b_{\perp}, P^z)|^2} + O(\alpha_s, (1/P^z)^2), \quad (9)$$

where power corrections from finite  $P^z$  are ignored. Since  $P^z$  is related to the rapidity of the meson, we henceforth replace it by the boost factor  $\gamma \equiv E_{\pi}/m_{\pi}$ . Eq. (7) can be written as

$$S_{I,\overline{\text{MS}}}(b_{\perp}, \mu) = \frac{F(b_{\perp}, P^z)}{F(b_{\perp,0}, P^z)} \frac{|\phi(0, b_{\perp,0}, P^z)|^2}{|\phi(0, b_{\perp}, P^z)|^2} + O(\alpha_s, \gamma^{-2}). \quad (10)$$

The ratio on the right-hand side of the above expression is independent of the renormalization scale  $\mu$  since only the leading-order contribution is kept.

On the other hand, the quasi-TMDWF can be used to extract the Collins-Soper kernel  $K$  using a method similar to [20]

$$K(b_{\perp}, \mu) = \frac{1}{\ln(P_1^z/P_2^z)} \ln \left| \frac{C(xP_2^z, \mu) \Phi_{\overline{\text{MS}}}(x, b_{\perp}, P_1^z, \mu)}{C(xP_1^z, \mu) \Phi_{\overline{\text{MS}}}(x, b_{\perp}, P_2^z, \mu)} \right| \quad (11)$$

$$= \frac{1}{\ln(P_1^z/P_2^z)} \ln \left| \frac{\int_0^1 dx \Phi(x, b_{\perp}, P_1^z)}{\int_0^1 dx \Phi(x, b_{\perp}, P_2^z)} \right| + O(\alpha_s, \gamma^{-2})$$

$$= \frac{1}{\ln(P_1^z/P_2^z)} \ln \left| \frac{\phi(0, b_{\perp}, P_1^z)}{\phi(0, b_{\perp}, P_2^z)} \right| + O(\alpha_s, \gamma^{-2}). \quad (12)$$

In the second line, again only the leading order matching kernel  $C(xP^z, \mu) = 1 + O(\alpha_s)$  is used. The renormalization factors for  $\Phi$  are cancelled. The rapidity-scheme-independent CS kernel  $K$  is independent of  $\mu$  in this approximation because only the leading term has been kept.

While Eqs. (7) and (11) are exact and can be used for precision studies in the future, Eqs. (10) and (12) are the leading-order approximation used in this pioneering work.

**Table 1:** Parameters used in the numerical simulation. The first row shows the parameters of the 2+1 flavor clover fermion CLS ensemble (named A654) and the second one shows the number of the A654 configurations and valence pion mass used for this calculation.

$\beta$	$L^3 \times T$	a (fm)	$c_{sw}$	$\kappa_l^{\text{sea}}$	$m_{\pi}^{\text{sea}}$ (MeV)
3.34	$24^3 \times 48$	0.098	2.06686	0.13675	333
			$N_{cfg}$	$\kappa_l^v$	$m_{\pi}^v$ (MeV)
			864	0.13622	547

### 3. Simulation Setup

For the present study, we use configurations generated with 2+1 flavor clover fermions and tree-level Symanzik gauge action configuration by the CLS collaboration using periodic boundary conditions [26]. The detailed parameters are listed in Table 1. Note that  $m_\pi = 547$  MeV instead of 333 MeV is used for valence quarks in order to have a better signal. Physically, the soft function becomes independent of the meson mass for large boost factors  $\gamma$ .

To calculate the form factor in Eq.(2), we generate the wall source propagator,

$$S_w(x, t, t'; \vec{p}) = \sum_{\vec{y}} S(t, \vec{x}; t', \vec{y}) e^{i\vec{p} \cdot (\vec{y} - \vec{x})}, \quad (13)$$

on the Coulomb gauge fixed configurations at  $t' = 0$  and  $t_{\text{sep}}$  for both the initial and final meson states.  $S$  is the quark propagator from  $(t', \vec{y})$  to  $(t, \vec{x})$ . Then we can construct the three point function (3pt) corresponding to the form factor in Eq. (2),

$$C_3(b_\perp, P^z; p^z, t_{\text{sep}}, t) = \frac{1}{L^3} \sum_x \text{Tr} \langle S_w^\dagger(\vec{x} + \vec{b}, t, 0; -\vec{p}) \gamma_5 \Gamma S_w(\vec{x} + \vec{b}, t, t_{\text{sep}}; \vec{p}) \times S_w^\dagger(\vec{x}, t, t_{\text{sep}}; -\vec{P} + \vec{p}) \gamma_5 \Gamma S_w(\vec{x}, t, 0; \vec{P} - \vec{p}) \rangle. \quad (14)$$

The quark momentum  $\vec{p} = (\vec{0}_\perp, p^z)$ , and the relation  $\gamma_5 S^\dagger(x, y) \gamma_5 = S(y, x)$  have been applied for the anti-quark propagator. We have tested several choices of  $\Gamma$ , and will use the unity Dirac matrix  $\Gamma = I$  as it has the best signal and describes the leading twist light-cone contribution in the large  $P^z$  limit. Notice that the  $\Gamma = \gamma_4$  case is subleading in the large  $P^z$  limit and is less suitable, although the excited state contamination might be smaller.

By generating the wall source propagators at all the 48 time slices with quark momentum  $p^z = (-2, -1, 0, 1, 2) \times 2\pi/(La)$ , we can maximize the statistics of the 3pt function with all the meson momenta  $P_z$  from 0 to  $8\pi/(La)$  ( $\sim 2.1$  GeV) with arbitrary  $t$  and  $t_{\text{sep}}$ .  $C_3(b_\perp, P^z, t_{\text{sep}}, t)$  is related to the bare  $F(b_\perp, P^z)$  using standard parameterization of 3pt with one excited state,

$$C_3(b_\perp, P^z; p^z, t_{\text{sep}}, t) = \frac{A_w(p_z)^2}{(2E)^2} e^{-Et_{\text{sep}}} [F(b_\perp, P^z) + c_1(e^{-\Delta Et} + e^{-\Delta E(t_{\text{sep}}-t)}) + c_2 e^{-\Delta Et_{\text{sep}}}], \quad (15)$$

$A_w$  is the matrix element of the Coulomb gauge fixed wall (CFW) source pion interpolation field,  $E = \sqrt{m_\pi^2 + P^z^2}$  is the pion energy,  $\Delta E$  is the mass gap between pion and its first excited state,  $c_{1,2}$  are parameters for the excited state contamination. Note that the  $p_z$  dependence factor  $A_w^2$  will cancel.

The same wall source propagators can be used to calculate the two-point function related to the bare quasi-TMDWF,

$$C_2(b_\perp, P^z; p_z, \ell, t) = \frac{1}{L^3 \sqrt{Z_E(2\ell, b_\perp)}} \sum_x \text{Tr} e^{i\vec{P} \cdot \vec{x}} \langle S_w^\dagger(\vec{x} + \vec{b}, t, 0; -\vec{p}) \mathcal{W}(\vec{b}, \ell) \gamma_5 \Gamma_\Phi S_w(\vec{x}, t, 0; P^z - \vec{p}) \rangle = \frac{A_w(p_z) A_p}{2E} e^{-Et} \phi_\ell(0, b_\perp, P^z, \ell) (1 + c_0 e^{-\Delta Et}), \quad (16)$$

where again we parameterize the mixing with one excited state.  $A_p$  is the matrix element of the point sink pion interpolation field. It will be removed when we normalize  $\phi_\ell(0, b_\perp, P^z, \ell)$  with

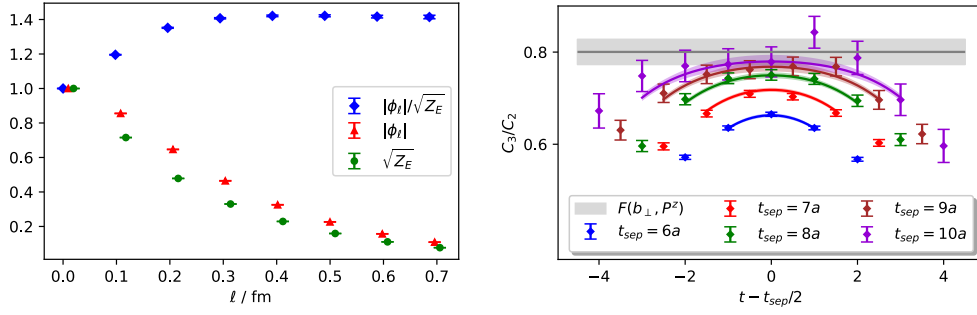


**Figure 1:** (a) Results for the  $\ell$  dependence of the quasi-TMDWF with  $z = 0$ , and also the square root of the Wilson loop which is used for the subtraction, taking the  $\{P^z, b_\perp, t\} = \{6\pi/L, 3a, 6a\}$  case as an example. All the results are normalized with their values at  $\ell = 0$ . (b) The ratios  $C_3(b_\perp, P^z, t_{\text{sep}}, t)/C_2(0, P^z, 0, t_{\text{sep}})$  (data points) which converge to the ground state contribution at  $t, t_{\text{sep}} \rightarrow \infty$  (gray band) as function of  $t_{\text{sep}}$  and  $t$ , with  $\{P^z, b_\perp\} = \{6\pi/L, 3a\}$ .

$\phi_\ell(0, 0, P^z, 0)$ . We choose  $\Gamma_\Phi = \gamma' \gamma_5$  to define the wave function amplitude in Eq. (4). Based on the quasi-TMDPDF study in Ref. [25, 27] with a similar staple-shaped gauge link operator, the mixing effect could be sizable when summing various contributions. We find that the mixing effects can reach order 5% for the transverse separation  $b_\perp \sim 0.6 \text{ fm}$ . These effects will be included in the following analysis as one of the systematic uncertainties, while a comprehensive study on the mixing effects will be conducted in the future.

#### 4. Numerical Results

Fig. 1(a) shows the dependence of the norm of quasi TMDWFs on the length  $\ell$  of the Wilson-line. As one can see from this figure, with  $\{P^z, b_\perp, t\} = \{6\pi/L, 3a, 6a\}$ , both the quasi-TMDWF  $\phi_\ell(0, b_\perp, P^z, \ell)$  and the square root of the Wilson loop  $Z_E$  decay exponentially with length  $\ell$ , but the subtracted quasi-TMDWF is length independent when  $\ell \geq 0.4 \text{ fm}$ . Based on this observation, we will use  $\ell = 7a = 0.686 \text{ fm}$  as asymptotic results for all cases in the following calculation.

We performed a joint fit of the form factor and quasi-TMDWF with the same  $P^z$  and  $b_\perp$  with the parameterization in Eqs. (15) and (16). The ratios  $C_3(b_\perp, P^z, t_{\text{sep}}, t)/C_2(0, P^z, 0, t_{\text{sep}})$  with different  $t_{\text{sep}}$  and  $t$  for the  $\{P^z, b_\perp\} = \{6\pi/L, 3a\}$  case are shown in Fig. 1(b), with ground state contribution (gray band) and the fitted results at finite  $t_2$  and  $t$  (colored bands). In this calculation, the excited state contribution is properly described by the fit with  $\chi^2/\text{d.o.f.} = 0.6$ . As shown in the plot, our data in general agree with the predicted fit function (colored bands).

The resulting soft factor as function of  $b_\perp$  is plotted in Fig. 2, at  $\gamma = 2.17, 3.06$  and  $3.98$ , which corresponds to  $P^z = \{4, 6, 8\}\pi/L = \{1.05, 1.58, 2.11\} \text{ GeV}$  respectively. As in Fig. 2, the results at different large  $\gamma$  are consistent with each other, demonstrating that the asymptotic limit is stable within errors. We also compare the intrinsic soft function extracted from the lattice to the one-loop result in Eq. (8), with  $\alpha_s(\mu = 1/b_\perp)$  evolving from  $\alpha_s(\mu = 2 \text{ GeV}) \approx 0.3$ . The shaded band corresponds to the scale uncertainty of  $\alpha_s$ :  $\mu \in [1/\sqrt{2}, \sqrt{2}] \times 1/b_\perp$ . Notice that the  $b_\perp$  dependence of the former comes purely from the lattice simulation, while that for the latter is from perturbation theory.

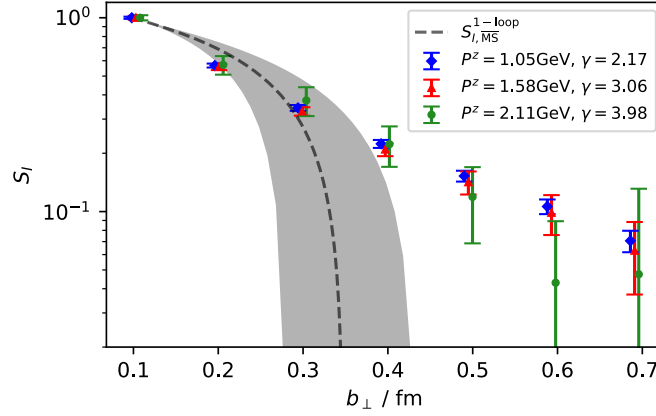


**Figure 2:** The intrinsic soft factor as a function of  $b_{\perp}$  with  $b_{\perp,0} = a$  as in Eq. (10). With different pion momentum  $P^z$ , the results are consistent with each other. The dashed curve shows the result of the 1-loop calculation, see Eq. (8), with the strong coupling constant  $\alpha_s(1/b_{\perp})$ . The shaded band corresponds to the scale uncertainty of  $\alpha_s$ :  $\mu \in [1/\sqrt{2}, \sqrt{2}] \times 1/b_{\perp}$ . The systematic uncertainty from the operator mixing has been taken into account.

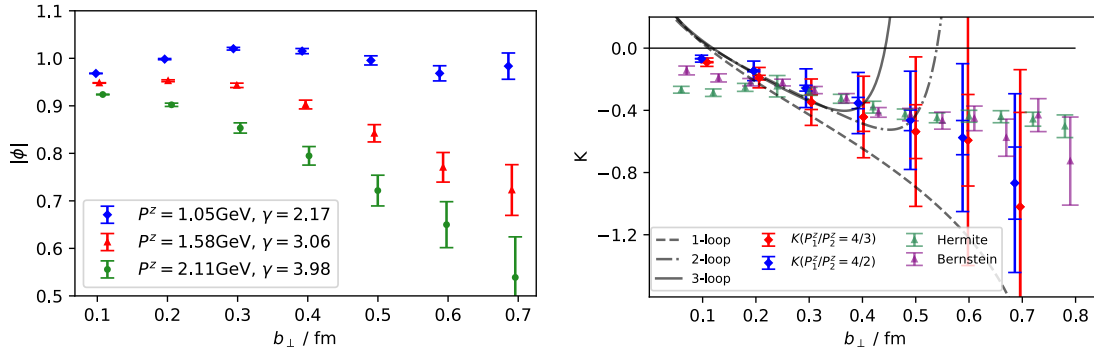


**Figure 3:** Quasi-TMDWF (left panel) and extracted Collins-Soper kernel (right panel), as functions of  $b_{\perp}$ . The visible  $P^z$  dependence of the quasi-TMDWF can be primarily understood by that from the Collins-Soper kernel, as the kernel we obtained with tree level matching is consistent with up to 3-loop perturbative calculations (at small  $b_{\perp}$ ) with the strong coupling  $\alpha_s$  at the scale  $1/b_{\perp}$ , and also the non-perturbative result from the pion quasi-TMDPDF. Results based on quenched lattice calculations, labeled as “Hermite” and “Bernstein” [25], are also shown for comparison. Errors in the lower panel correspond to the statistical errors and the systematic errors from the non-zero imaginary part as well as the operator mixing effects.

We can see a clear  $P^z$  dependence in the quasi-TMDWF  $|\phi_{\ell}(0, b_{\perp}, P^z, \ell)|$  normalized with  $\phi_{\ell}(0, 0, P^z, 0)$ , as in the left panel of Fig. 3. This dependence is related to the CS kernel as shown in Eq. (12), up to possible LaMET matching effects and power corrections of order  $1/\gamma^2$ . Thus we use Eq. (12) to extract the kernel in the tree level approximation, and compare the result in the right panel of Fig. 3 with that of Ref. [25] and up to 3-loop perturbative ones with  $\alpha_s(\mu = 1/b_{\perp})$ . We estimate the systematic uncertainty by combining in quadrature the contributions from the operator mixing effects, and from the non-vanishing imaginary part of the quasi-TMDWF which should be



cancelled by proper treatments on higher order effects. Our result is consistent with that of Ref. [25].

## 5. Summary and Outlook

In this work, we have presented an exploratory lattice calculation of the intrinsic soft function by simulating the light-meson form factor of four-quark non-local operators and quasi-TMD wave functions. Our result shows a mild hadron momentum dependence, which allows a future precision study to eliminate the large momentum dependence using perturbative matching [16]. As a reliability check, the agreement between the CS kernel obtained from our quasi-TMDWF result and previous calculations shows that the systematic uncertainties including the partially quenching effect, the only leading perturbative matching and missing power corrections  $1/\gamma$  in LaMET expansion might be sub-leading. Our calculation paves the way towards the first principle predictions of physical cross sections for, e.g., Drell-Yan and Higgs productions at small transverse momentum.

## Acknowledgments

We would thank Xu Feng, Yuan Li, Shi-Cheng Xia, Jianhui Zhang and Yong Zhao for valuable discussions, and thank the CLS Collaboration for sharing the lattice ensembles used to perform this study. This work is supported by National Natural Science Foundation of China under the Grant No.12005130, 11735010, 11947215, 11975127, 11735010 and 11911530088. MS and AS are supported by the cooperative research center CRC/TRR-55 of DFG, PS is supported by Jiangsu Specially Appointed Professor Program, WW is supported by Natural Science Foundation of Shanghai under grant No. 15DZ2272100 and QAZ is supported by the China Postdoctoral Science Foundation and the National Postdoctoral Program for Innovative Talents (Grant No. BX20190207).

## References

- [1] R. K. Ellis, W. J. Stirling, and B. R. Webber, *Camb. Monogr. Part. Phys. Nucl. Phys. Cosmol.* **8**, 1 (1996).
- [2] H.-W. Lin *et al.*, *Prog. Part. Nucl. Phys.* **100**, 107 (2018), [arXiv:1711.07916 \[hep-ph\]](#) .
- [3] J. C. Collins and D. E. Soper, *Nucl. Phys.* **B193**, 381 (1981), [Erratum: *Nucl. Phys.*B213,545(1983)].
- [4] J. C. Collins, D. E. Soper, and G. F. Sterman, *Nucl. Phys.* **B250**, 199 (1985).
- [5] X.-d. Ji, J.-p. Ma, and F. Yuan, *Phys. Rev.* **D71**, 034005 (2005), [arXiv:hep-ph/0404183 \[hep-ph\]](#) .
- [6] X.-d. Ji, J.-P. Ma, and F. Yuan, *Phys. Lett.* **B597**, 299 (2004), [arXiv:hep-ph/0405085 \[hep-ph\]](#) .
- [7] M. G. Echevarria, I. Scimemi, and A. Vladimirov, *Phys. Rev.* **D93**, 054004 (2016), [arXiv:1511.05590 \[hep-ph\]](#) .



- [8] Y. Li and H. X. Zhu, *Phys. Rev. Lett.* **118**, 022004 (2017), arXiv:1604.01404 [hep-ph] .
- [9] X. Ji, Y. Liu, and Y.-S. Liu, (2019), arXiv:1910.11415 [hep-ph] .
- [10] X. Ji, *Phys. Rev. Lett.* **110**, 262002 (2013), arXiv:1305.1539 [hep-ph] .
- [11] X. Ji, *Sci. China Phys. Mech. Astron.* **57**, 1407 (2014), arXiv:1404.6680 [hep-ph] .
- [12] J. Collins, *Camb. Monogr. Part. Phys. Nucl. Phys. Cosmol.* **32**, 1 (2011).
- [13] C. W. Bauer, S. Fleming, D. Pirjol, and I. W. Stewart, *Phys. Rev.* **D63**, 114020 (2001), arXiv:hep-ph/0011336 [hep-ph] .
- [14] C. W. Bauer and I. W. Stewart, *Phys. Lett.* **B516**, 134 (2001), arXiv:hep-ph/0107001 [hep-ph] .
- [15] C. W. Bauer, D. Pirjol, and I. W. Stewart, *Phys. Rev.* **D65**, 054022 (2002), arXiv:hep-ph/0109045 [hep-ph] .
- [16] X. Ji, Y.-S. Liu, Y. Liu, J.-H. Zhang, and Y. Zhao, (2020), arXiv:2004.03543 [hep-ph] .
- [17] K. Cichy and M. Constantinou, *Adv. High Energy Phys.* **2019**, 3036904 (2019), arXiv:1811.07248 [hep-lat] .
- [18] X. Ji, P. Sun, X. Xiong, and F. Yuan, *Phys. Rev.* **D91**, 074009 (2015), arXiv:1405.7640 [hep-ph] .
- [19] X. Ji, L.-C. Jin, F. Yuan, J.-H. Zhang, and Y. Zhao, *Phys. Rev.* **D99**, 114006 (2019), arXiv:1801.05930 [hep-ph] .
- [20] M. A. Ebert, I. W. Stewart, and Y. Zhao, *Phys. Rev.* **D99**, 034505 (2019), arXiv:1811.00026 [hep-ph] .
- [21] M. A. Ebert, I. W. Stewart, and Y. Zhao, *JHEP* **09**, 037 (2019), arXiv:1901.03685 [hep-ph] .
- [22] X. Ji, Y. Liu, and Y.-S. Liu, (2019), arXiv:1911.03840 [hep-ph] .
- [23] A. A. Vladimirov and A. Schäfer, *Phys. Rev.* **D101**, 074517 (2020), arXiv:2002.07527 [hep-ph] .
- [24] M. A. Ebert, I. W. Stewart, and Y. Zhao, *JHEP* **03**, 099 (2020), arXiv:1910.08569 [hep-ph] .
- [25] P. Shanahan, M. Wagman, and Y. Zhao, (2020), arXiv:2003.06063 [hep-lat] .
- [26] M. Bruno *et al.*, *JHEP* **02**, 043 (2015), arXiv:1411.3982 [hep-lat] .
- [27] P. Shanahan, M. L. Wagman, and Y. Zhao, *Phys. Rev.* **D101**, 074505 (2020), arXiv:1911.00800 [hep-lat] .